ORIGINAL PAPER

Assessment of long-term structural movements in a historic cliffside construction through Lomb-Scargle spectral analysis of unevenly spaced time records: the Punta Begoña Galleries (Getxo, Spain)

J. A. Uriarte[1] · R. Morales-Juberías[2] · J. A. Clemente[1] · I. Antiguedad[1] · T. Morales[1]

Abstract

Long-term monitoring of structural movements in historic buildings and heritage sites allows assessing their stability and recognizing damages that require intervention. The Punta Begoña Galleries, built in the earlier part of the twentieth century, present pioneering techniques in the use of reinforced concrete in building construction. They stand directly over a coastal cliff, and their recovery requires first to guarantee their stability, while maintaining their historic and patrimonial values. Thus, with the goal of analyzing their global stability, as well as the extent of the observed damages, we implemented a motion monitoring network that includes three boreholes for extensometric control, an inclinometer, and five crack gauges (crackmeters). This monitoring was complemented with the recording of hydrometeorological variables at the surface and in four piezometers. The spectral analysis of the signals of movements was performed by introducing the use of the Lomb-Scargle (LS) periodogram, which is particularly well-suited for the analysis of unevenly spaced time series. This analysis allowed us to differentiate the reversible seasonal elastic components of the records and to recognize the irreversible long-term plastic displacements, which highlight the sectors with active instability. In our case, the identified damages are related to two local problems of building support. Even though the irreversible component of the displacement after seasonal sinusoidal detrending is small (with maximums up to 0.12 mm/year), it does imply a dynamic plastic deformation, which calls for the need to adopt structural stabilization measures.

Keywords Heritage sites stability · Long-term monitoring · Lomb-Scargle periodogram · Damage assessment · Conservation plan

Introduction

Conservation and stabilization projects in environments of well-known cultural relevance not only must address the repairs of any existing damages, but also must ensure the preservation of the historical value of the site (Guo et al. 2009). Thus, and following the recommendations compiled in the "ICOMOS Charter – Principles for the analysis, conservation and structural restoration of architectural heritage (2003)," the rehabilitation measurements aim to address the root of the problems while being minimally invasive in order to guarantee the safety and durability of the site and to mitigate damage to the patrimony.

Consequently, the diagnosis and knowledge of both the building techniques and the processes of alteration and structural damages are fundamental to rehabilitate and repurpose the historic building (Heinemann 2008, 2013; ICOMOS 2010, 2014; Laborde Marqueze 2013; Custance-Baker and Mac Donald 2014). The diagnosis must follow specific methodologies in order to understand the structure and building methods, to characterize the alteration processes, and to evaluate and control the structural safety of the site (Chang et al. 2003; ICOMOS 2003; Heinemann 2008; Laborde Marqueze 2013; Damas Mollá et al. 2018, 2020). For cultural heritage and archeological sites considered to be affected by geologically based issues and geohazards, monitoring strategies incorporate a wide range of

✉ J. A. Uriarte
jesus.uriarte@ehu.eus

1 Department of Geology, Faculty of Science and Technology, University of the Basque Country UPV/EHU, P.O. Box 644, E-48080 Bilbao, Spain

2 Physics Department, New Mexico Institute of Mining and Technology, Socorro, NM 87801, USA

complementary survey techniques (Margottini et al. 2015; Themistocleous and Danezis, 2019), including, at the local-scale (Themistocleous et al. 2018), in situ observation, 3D laser scanning, differential GNSS, satellite and ground-based radar interferometry, UAV imagery (Colomina and Molina 2014; Tang et al. 2016), along with geotechnical instrumentation for displacement control, mainly extensometers and crack gauges (Ding et al. 2000; Greif et al. 2006; Mulas et al. 2020), and environmental sensors.

It is within this framework that we approach the recovery and revalorization of the Punta Begoña Galleries (Getxo, Spain). Previous reports question the overall stability of this early twentieth century building. The stability of its most significant spaces, namely the Northwest and Southwest Galleries, in relation to the stability of the cliff upon which they were built was highly questioned, leading to pose the need to demolish the building and only preserve architectural elements of the façade. In this context, given the local development of the damage observed, and the fact that these are extremely slow movements, in the sense that they do not pose an immediate threat to the structure, but have proven to be detrimental over the long course of time (Greif et al. 2006), a permanent geotechnical recording system (Cempel 2003; De Stefano et al. 2016) was designed in order to monitor the instability symptoms. This geotechnical monitoring system is chiefly based on wire extensometers and crack gauges seeking to identify the behavior of this dual context in which the development of instabilities in the cliff can lead to the development of damage to the building's structure, whose supports in turn alter the state of the terrain's original stresses.

Records from these devices are affected by temperature changes giving rise, due to material's thermal dilatancy, to opening-closing cycles in the time series that can mask significant and worrisome small irreversible displacements (Weber et al. 2017; Janeras et al. 2017; Mulas et al. 2020). To separate these reversible (elastic) components from the signals and quantify the irreversible (plastic) displacements, Weber et al. (2017) have proposed a linear fit method between temperature and fracture opening. This approach requires temperature series, so Mulas et al. (2020) propose a sinusoidal wave fit of displacement time series, avoiding the consideration of temperature series that may lead to biased results as they observed significant timelag of the temperature signal with depth. In this work, we introduce the use of the Lomb-Scargle spectral analysis of the time series (Lomb 1976; Scargle 1982). The Lomb-Scargle analysis can be understood as a *Least-Squares Spectral Analysis* (LSSA) method. This technique was originally developed for the analysis of astronomical time series, but it has been adopted to analyze time series in different geology fields such as environmentology, climatology and paleoclimatology (Pestiaux and Berger 1984; Schulz and Stattegger 1997;

Hocke and Kampfer 2009), seismology (Park et al. 1987), and cyclostratigraphy (Weedon 2003; Pardo-Igúzkiza and Rodríguez-Tovar 2011; Vaughan et al. 2015). The main advantage of this method is the ability to overcome the limitations imposed by other methods that require continuous and evenly spaced time series; thus, this method eliminates the need to fill unevenly sampled time series with interpolated values, which can have an effect on the spectral analysis results (Schulz and Stattegger 1997; Pardo-Igúzkiza and Rodríguez-Tovar 2012).

Our main objective is to analyze the efficiency of the installed monitoring network, as the basis of a cliff and structural health monitoring system, and to show how the Lomb-Scargle spectral analysis can be used to quantify the magnitude of the instabilities and the scope of the damages. This information will be essential for the design of mitigation strategies that would preserve the natural and cultural value of the cliff-structure complex, while incorporating the necessary safety measures for its public use.
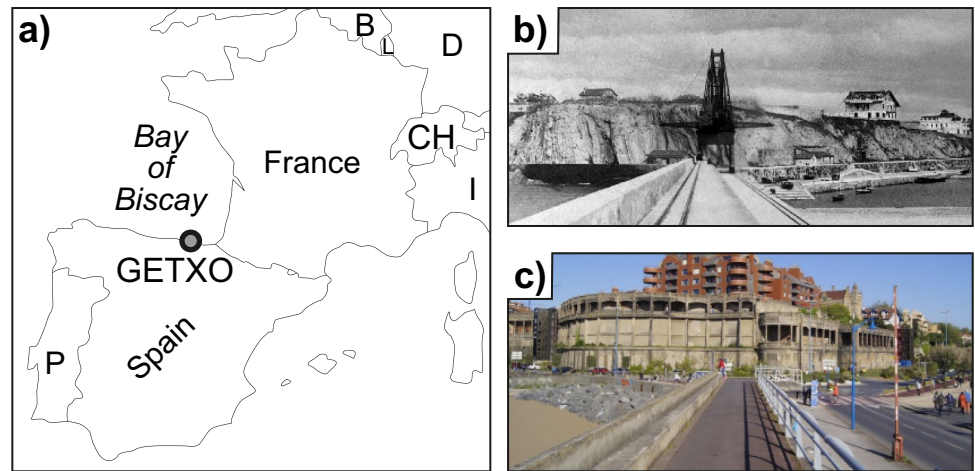
Construction context

The Punta Begoña Galleries are located in the municipality of Getxo, on the coastal cliffs of this sector of the Bay of Biscay (Fig. 1). Designed by Ricardo Bastida as an extension of Horacio Etxevarrieta's house, the galleries were built directly on the rocky wall of the cliff, constituting a watchtower over the entrance of Bilbao's Estuary.

From a geological point of view, materials outcropping in this sector of the coast are Mesozoic and Cenozoic successions of marine deposits folded during the Alpine Orogeny (Morales et al. 2004). In the area where the galleries were built, these materials show a flyschoid alternation, consisting of hemipelagic marls and marly limestones (Upper Cretaceous gray and red marls and marly limestones). The arrangement of rock strata shows a northwest-southeast direction dipping deeply towards the south.

In this geological context, Punta Begoña Galleries were built at the beginning of the twentieth century, adapting its shape and structure to the morphology of the cliff (Fig. 1b, c). Their origin appears to be related to a rockfall that made necessary the stabilization of the area. The architect Ricardo Bastida designed, for this purpose, a wall with out-facing pavilions in 1918, which eventually resulted, in 1921, in a more ambitious construction: the current galleries. The final building structure resulted in two main façades that are perpendicular to each other: the so-called Northwest Gallery, with a large room, called the Hall, followed by an elevated corridor; and the Southwest Gallery (Fig. 2a). The galleries are separated by a semicircular structure, known as the "Tholos" that acts as a juncture.

Fig. 1 **a** Geographical location. **b** Image prior to construction. **c** Punta Begoña Galleries today

Their construction coincided with the beginning of the use of reinforced concrete (Rosell and Cárcamo 1994; Díaz Morlán 1999, 2011). The façades are based on a sandstone masonry wall (Fig. 2b, d), on which an intermediate section of reinforced concrete blind wall was built. The blind wall supports a corridor gallery with concrete columns and prefabricated balustrades, crowned by an upper garden. The pillars of the structure are also made of reinforced concrete and were built directly on the original cliff (Fig. 2c, e, and f), resting on small footings excavated in a staggered manner. An important aspect to highlight is the differing relationship between the rocky cliff and the structure of the building on both façades. Namely, while the orientation of the Northwest Gallery façade is perpendicular to the direction of the strata

Fig. 2 **a** Plan of the Punta Begoña Galleries. **b** Exterior of the Northwest Gallery Hall. **c** Interior space underneath The Hall, showing the pillars standing on the cliffside. **d** and **e** Exterior of the Southwest Gallery. **f** Interior showing the supporting pillars over the chalky strata. S_0, stratification
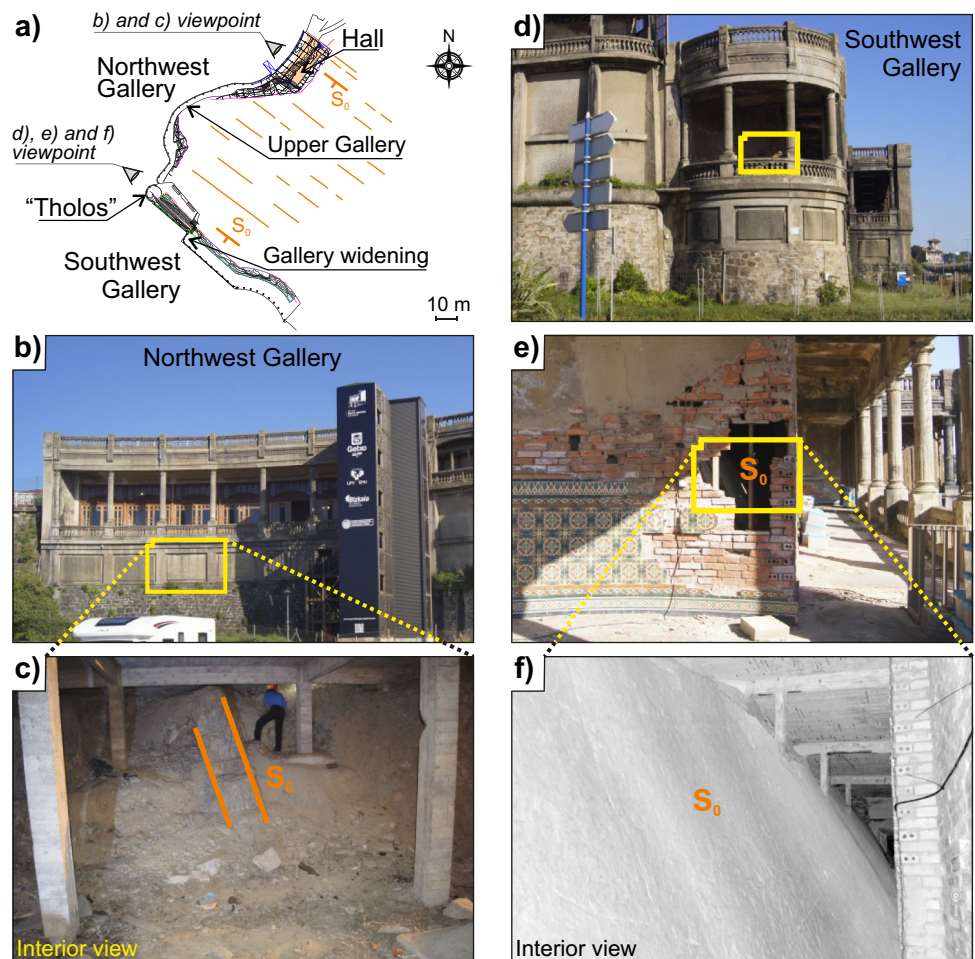
(Fig. 2c), the direction of the stratification and the façade of the Southwest Gallery are parallel (Fig. 2e, f).

Consequently, after years of neglect, when in 2014, the Getxo City Council promoted the recovery and enhancement of this heritage site; it emerged as a priority issue to establish the nature and extent of the damages to the building. Initially, its general stability in relation to the cliff-construction interaction was particularly questioned, so a monitoring strategy was designed with the aim of measuring and assessing the observed damage.

Methodology

Movement control network

As a first step, in order to have a highly accurate digital reference to include the different observations of the building, we created a geometrical model of the building and its supports in the rocky slope. For this, a Terrestrial Laser Scanner (TLS), with a FARO Laser Scanner Focus 3D X330 equipment, was used to make a full scanning of the building and the rocky slope. The TLS is an ideal technique for buildings with irregular and not very accessible morphologies (Casula et al. 2009; Montuori et al. 2014; Dong et al. 2020). The 3D Point Cloud (3DPC) clearly depicts both the detailed structure of the building and the cliff. The 3DPC is essential for the detailed management of high-value heritage elements, before acting on them. In our project, the software Web Share 2 Go (FARO 3D Visionary) enabled real viewing of the scanned space through an external cloud service, which allowed us to make measurements. We completed planimetrics based on the 3DPC point cloud using CAD software.

Based on this planimetric model, and after reviewing the building's structural damages, we set up the movement monitoring network together with a hydrogeological control system (Fig. 3):

Northwest gallery

The area known as "the Hall" is located here. This is the area where most activity is registered by researchers and where the main social and outreach events take place, including thematic workshops and some of the most attended activities open to the public, such as the regular venue for the International Image Festival Getxofoto (www.getxophoto.com).

In this façade (Fig. 4a), despite the orientation of the strata being perpendicular to the slope, and therefore favorable for stability, previous reports identified a crack, with a maximum aperture of 1 cm, in the upper concrete slab at its northeastern corner (Fig. 4b), coinciding with the access stairway to the building from the upper esplanade. This observation was interpreted as a sign of global instability of

the building in relation to the cliff, so the first extensometer set (EXT-1) was installed in 2014 from the lower masonry wall of the galleries (Fig. 4a). For this purpose, an 11-m deep horizontal drilling was carried out, with a diameter of 101 mm for the first 3.60 m, and of 86 mm for the remaining depth. This drilling went through 1.20 m of wall, clayey fills of anthropic nature up to 3.40 m deep, 0.20 m of fragmented rock without matrix, and marly rocks and marly limestones up to the end of the drilling. We then performed the extensometric control by placing 2 potentiometric sensors arranged in an external head, with two sets of rods fixed with hydraulic anchors (Fig. 3a): from 2.50 to 3.25 m (short rod) and from 10.00 to 10.75 m (long rod), respectively (Fig. 4a). The measuring range of the IKM potentiometers (DPF Sensors) is 50 mm, with an accuracy of ± 0.01 mm. A Campbell Scientific CR200X Series datalogger recorded, at the desired time step, environmental temperature, and ground movements on both rods. The frequency of data recording has varied throughout the research period, as needed, from hourly to every 4 to 12 h.

Slightly further south, in the most prominent zone of the original cliff, and therefore of the building, we decided (in 2016) to perform one inclinometric drilling (INC-1) from the upper esplanade. The borehole reaches a depth of 21 m, with a diameter of 101 mm. Initially, it passed through 1.20 m of loose material and fill before reaching the rock massif, consisting of an alternation of marls and marly limestones. This borehole was equipped with an inclinometric pipe. The inclinometric measurements were made with a Soil Instruments C17-pro biaxial probe with a monthly periodicity, which allows quantifying the relative horizontal movements on a vertical line.

At the same time, we installed a hydrogeological monitoring system (Fig. 4a), consisting of two piezometers, one located on the upper terrace of the building (SP-3 piezometer) and the other at its base (SP-1 piezometer). Each of these piezometers was equipped with water temperature, water level, and electric conductivity control devices (CTD-Divers) from the brand Schlumberger. In both boreholes, barometric devices were also installed at 20 cm depth to record air temperature and pressure. Figure 4 shows the monitoring network in the area around the Hall.

Southwest gallery

Unlike in the Northwest Gallery, the direction of the façade in the southwest side of the building is parallel to the stratification. The stability of this gallery was compromised as part of the structure was loaded on the original cliff strata (Figs. 2f and 5a). In fact, the Southwest Gallery is the sector that shows the main damages, including several cracks affecting its structure, particularly in two well-localized sectors: the "Tholos," with a maximum crack aperture of
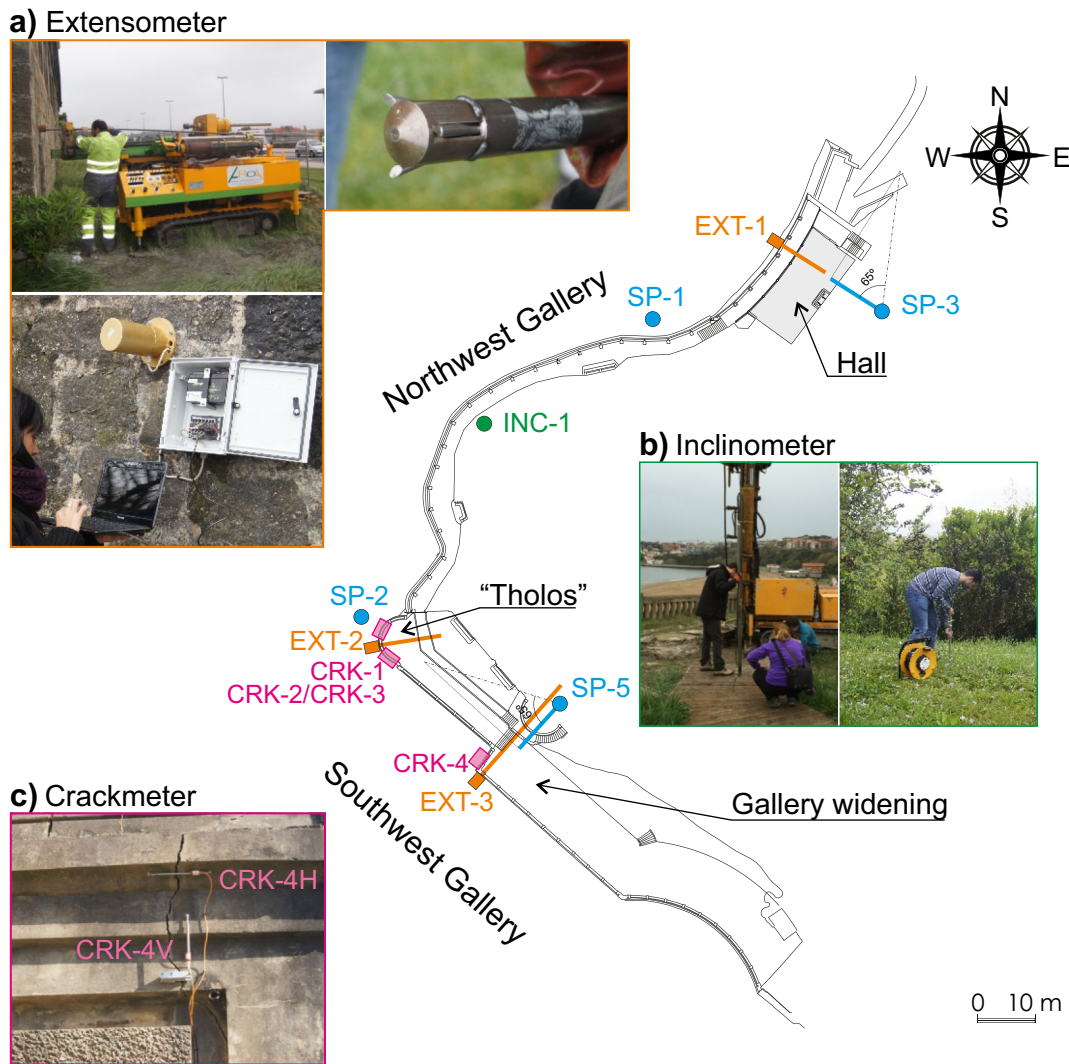
Fig. 3 Movement control and hydrogeological monitoring devices in Punta Begoña Galleries. Equipment installation: **a** extensometers, **b** inclinometer, and **c** crackmeters. EXT, borehole for extensometric control; CRK, crackmeter; INC, inclinometer; SP, piezometer

1 cm (Fig. 5d), and the section where the gallery widens, in which cracks reach 2 cm of aperture in the upper terrace (Fig. 5b) and up to 1 cm in other parts of the building, as in the façade (Fig. 5c).

With the aim of analyzing the evolution of damages in both sectors, two extensometric control units were implemented in 2014 (EXT-2) and 2016 (EXT-3). The extensometer set EXT-2 was located in the "Tholos" (Figs. 3 and 5). To install it, we carried out a horizontal drilling of 9 m in length and a diameter of 101 mm for the first 1.10 m, and 86 mm for the rest of its length. After 1.30 m of masonry wall, we reached the marls and marly limestones of the rock massif on which the "Tholos" rests. Two potentiometric measurement sensors were installed, with the technical characteristics previously indicated, as well as two sets of rods with hydraulic anchors from 2.5 to 3.25 m (short rod) and 8.00 to 8.75 m (long rod), respectively.

The extensometer set EXT-3 was installed in the outer façade corner where the Southwest Gallery widens (Fig. 3). For this purpose, a 20.80 m horizontal drilling was made, with a diameter of 101 mm along its entire length. Due to its parallel disposition to the wall, it ran along the wall for 5.30 m, where it reached the marls and marly limestones of the rocky substrate on which the corner rests. The control equipment has a head with two OG400VW vibrating wire sensors (OTR) and two sets of rods with hydraulic anchors fixed from 10.00 to 10.75 m and from 19.50 to 20.25 m, respectively. The measurement range of these sensors is 50 mm, with an accuracy of ± 0.1 mm. The Geosense Geologger LINX data logger continuously records the environmental temperature and the movements of both rods. The periodicity of data acquisition was varied as needed.

In order to monitor the activity of the main cracks in this gallery, five crackmeters were installed: three KLR

Fig. 4 **a** Schematic cross-section of the Point Cloud of the Punta Begoña Galleries in the Hall, with the location of the EXT-1 extensometer, SP-1 and SP-3 piezometric boreholes. **b** Image of the existing crack in the upper slab of the building
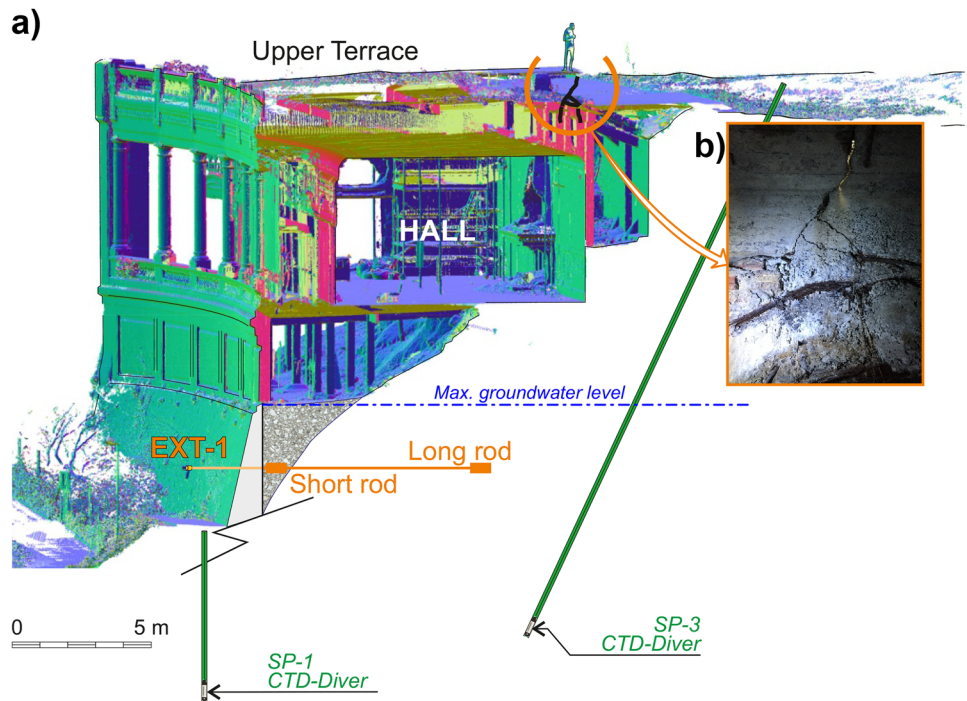
potentiometric ones (Novotechnik) at the "Tholos" (CRK-1, CRK-2, and CRK-3), with an accuracy of ± 0.05 mm; and two VWDT vibrating wire (Geosense VW) on the façade where the Southwest Gallery widens, with an accuracy

of ± 0.05 mm, named CRK-4H and CRK-4 V (set CRK-4). The data were recorded in the same data loggers that collected the extensometric information and with the same periodicity, ranging from 1 to 12 h increments.

Fig. 5 **a** Schematic cross-section of the Point Cloud of the Punta Begoña Galleries in the "Tholos" and Southwest Gallery. **b** and **c** Images of the main cracks in the section where the gallery widens. **d** Main crack in the "Tholos" façade
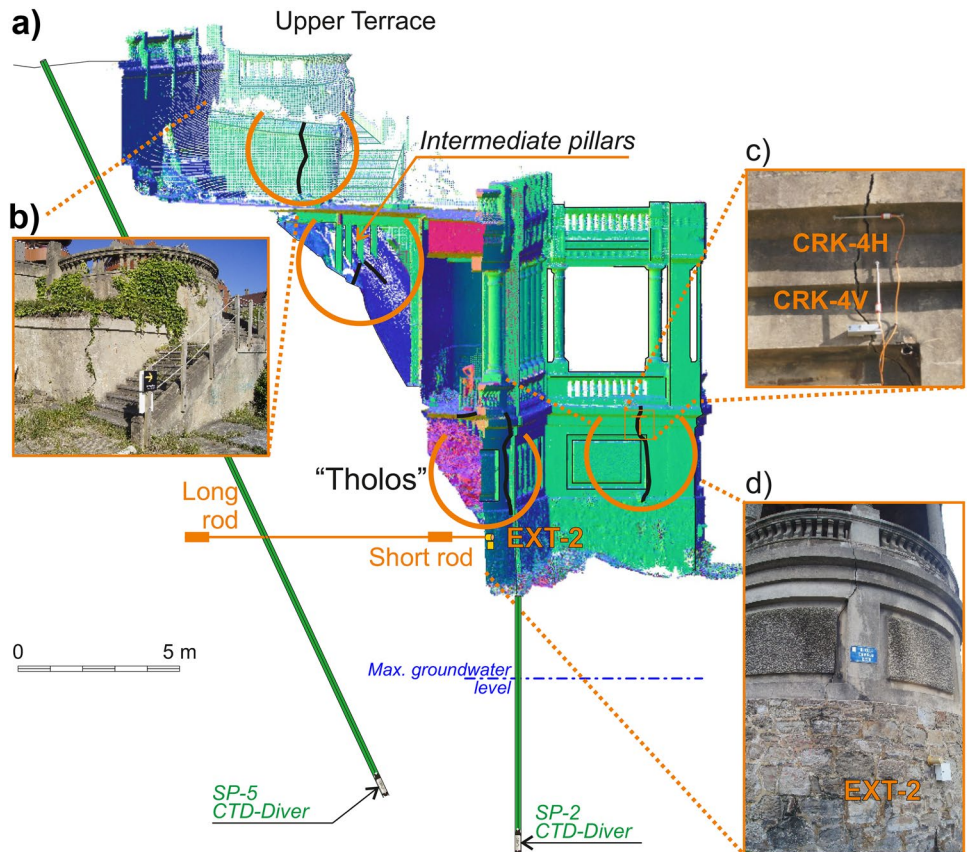
Monitoring in this sector was also completed with two piezometers (Fig. 5), one in the upper terrace (SP-5) and the other at the foot of the galleries (SP-2).

Spectral analysis of data series

From the information obtained in the field campaign, we used the time series analysis to differentiate between the reversible tendencies characterized by cyclic components, representative of elastic behavior, and the irreversible tendencies that would point to the existence of plastic deformations.

To this end, after importing the data with the *pandas* data analysis tool (McKinney 2010; Reback et al. 2020), first we performed a least-squares linear fit to all the signals to remove any linear trend. After removing the linear trends and the mean from our signals, we performed a spectral analysis using the Lomb-Scargle method (Lomb 1976; Scargle 1982) to identify the most dominant periods of cyclic reversible changes. To perform the calculation of the periodogram, we used the *gastpy* package developed by VanderPlas and Ivezić (2015). Specifically, we use the fast periodogram implementation based on the algorithm developed by Press and Rybicki (1989).

For a data series x_n sampled at nonuniform times t_n, the expression for the Lomb-Scargle periodogram is given by:

$$P_{LS}(f) = \frac{1}{2}\left\{ \frac{\left(\sum_n x_n \cos\left(2\pi f\left[t_n - \tau\right]\right)\right)^2}{\sum_n x_n \cos^2\left(2\pi f\left[t_n - \tau\right]\right)} + \frac{\left(\sum_n x_n \sin\left(2\pi f\left[t_n - \tau\right]\right)\right)^2}{\sum_n x_n \sin^2\left(2\pi f\left[t_n - \tau\right]\right)} \right\}, \tag{1}$$

where f is the frequency and τ is an offset specified for each frequency to ensure time-shift invariance:

$$\tau = \frac{1}{4\pi f}\tan^{-1}\left(\frac{\sum_n \sin\left(4\pi f t_n\right)}{\sum_n \cos\left(4\pi f t_n\right)} \right) \tag{2}$$

When written in this form, the expression for the periodogram resembles that of the classical periodogram of evenly sampled data using the Fourier transform. The Lomb-Scargle method can also be interpreted in terms of a least-squares fit to a sinusoidal function at each frequency of the form:

$$y(t,f) = A_f \sin\left(2\pi f\left(t - \varphi_f\right)\right) \tag{3}$$

where the amplitude A_f and the phase φ_f parameters can vary as a function of frequency and are fitted to the data using a least-squares method (VanderPlas 2018). In our case, we use:

$$y(t,f) = A_0 + A_f \sin\left(2\pi f\left(t - \varphi_f\right)\right) \tag{4}$$

where A_0 is the average value of the oscillation, which depends on the initial setting of the equipment.

Results

Monitoring data

In this section, we present the results obtained from the crackmeter set CRK-4, and extensometers EXT-1 and EXT-2, which are the three control units that provided the most significant information regarding the cliff-building stability. In order to allow for a comparative view of the data registered by these instruments, in Fig. 6, we include the direct observations obtained from 2015 to 2019.

Thus, in Fig. 6a, we show the data from the crackmeter set CRK-4, which registers the horizontal (CRK-4H) and vertical (CRK-4 V) displacements in the façade's main crack in the sector where the Southwest Gallery widens (Fig. 5c). Both signals show a clear periodicity, with a peak-to-peak amplitude of 0.566 mm for the horizontal displacement (CRK-4H) and of 0.403 mm for the vertical displacement (CRK-4 V). In this figure, we also show the variation in ambient temperature recorded in the nearby weather station of Punta Galea (Getxo). The daily average temperatures also show a clear seasonal tendency, with highs of up to 25 °C during the summertime and lows of 5 °C during the wintertime. As can be seen, the displacements in the crack show a logical inverse relationship with the ambient temperature (Mulas et al. 2020), with maximum crack openings corresponding to colder periods, and crack closing during the warmest months, in relation to the thermal retraction-dilatation processes of the facade materials, respectively.

In Fig. 6b, we present the data from the extensometer EXT-1 in the Northwest Gallery (Fig. 4), those obtained by the rod anchored between 10.00 and 10.75 m (long rod) and those obtained by the rod anchored between 2.50 and 3.25 m depth (short rod). These signals show a clearer cyclicality, with a peak-to-peak amplitude of 0.533 mm for the long rod and 0.723 mm for the short one. We note that during the first year and a half, the long rod showed a relatively static behavior (Fig. 6b), but after replacing the sensor, its measurements were similar in magnitude and direction to those obtained from the short rod. In both cases, the largest elongation of the rods corresponds to the winter time. This apparently paradoxical behavior can be explained taking into account the offset of the temperature evolution inside the ground. In order to clearly show this evolution,
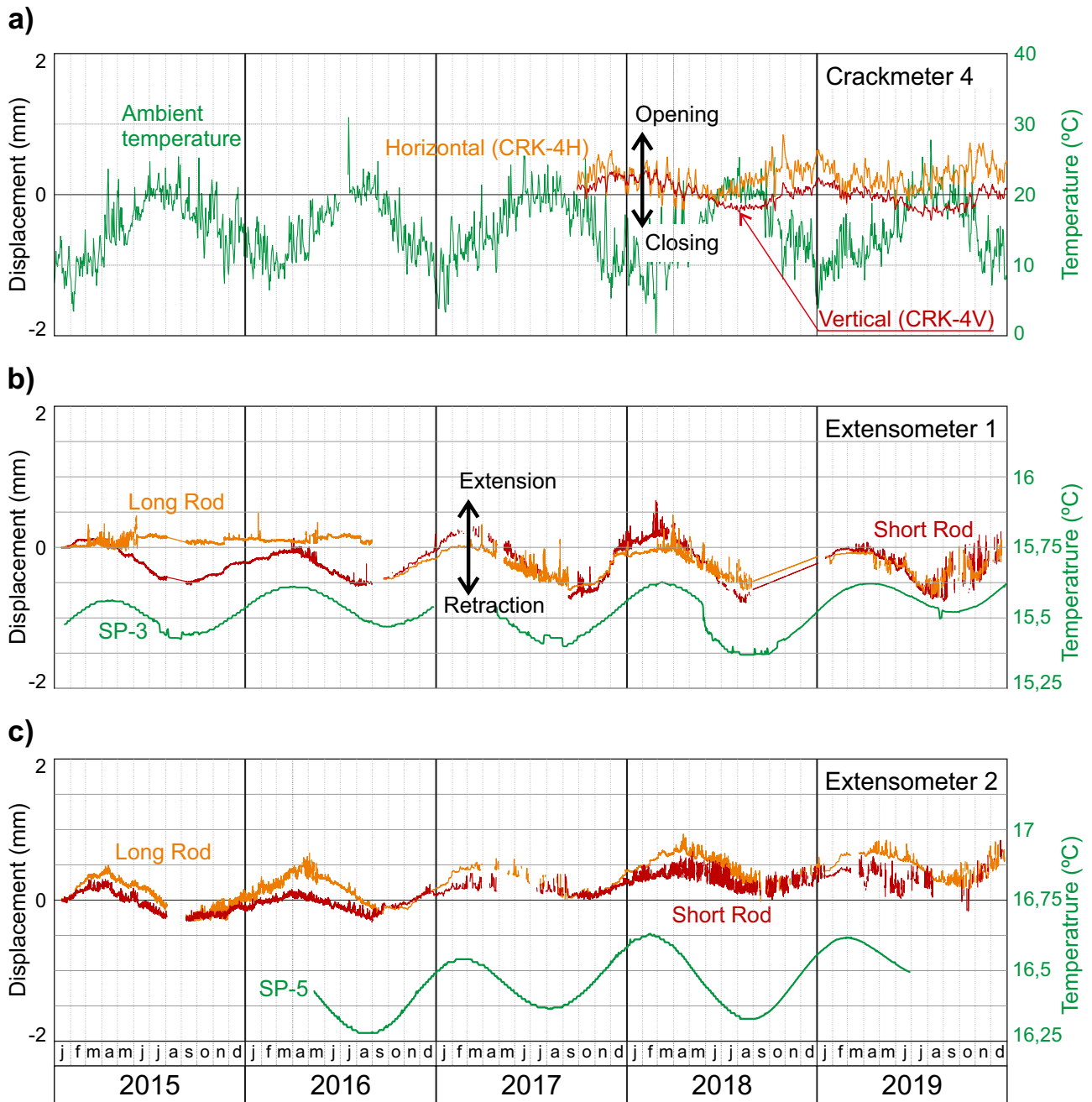
Fig. 6 Records from 2015 to 2019: **a** crackmeter CKR-4, horizontal (CRK-4H) and vertical (CRK-4 V) movements, together with the ambient temperature at Punta Galea weather station; **b** extensometer EXT-1 long rod (anchored at 10.00 to 10.75 m depth) and short rod (anchored from 2.50 to 3.25 m depth), together with temperature evolution at SP-3; **c** extensometer EXT-2 long rod (anchored at 8.00 to 8.75 m depth) and short rod (anchored from 2.5 to 3.25 m depth), together with temperature at SP-5 piezometer

Fig. 7 shows the standardized records of ambient temperature, air temperature at 20 cm depth in the SP1 piezometer (measured by the barometric device), and water temperatures recorded by the CTD-divers in the piezometers SP-1, SP-2, SP-3, and SP-5. This figure clearly shows how there is essentially no noticeable offset between the ambient temperature and the air temperature inside the piezometer, and

how the latter is a smoother version of the former. Regarding the piezometers located at the base of the building, Fig. 7 (panels a and b) shows how the water temperatures recorded at depths of 6.1 m and 8.6 m in the piezometers SP-1 and SP-2 exhibit lags of 80 to 106 days with respect to the previous signals, and a clear incidence of the arrival of rainwater in the records. Finally, the CTD-divers located at depths
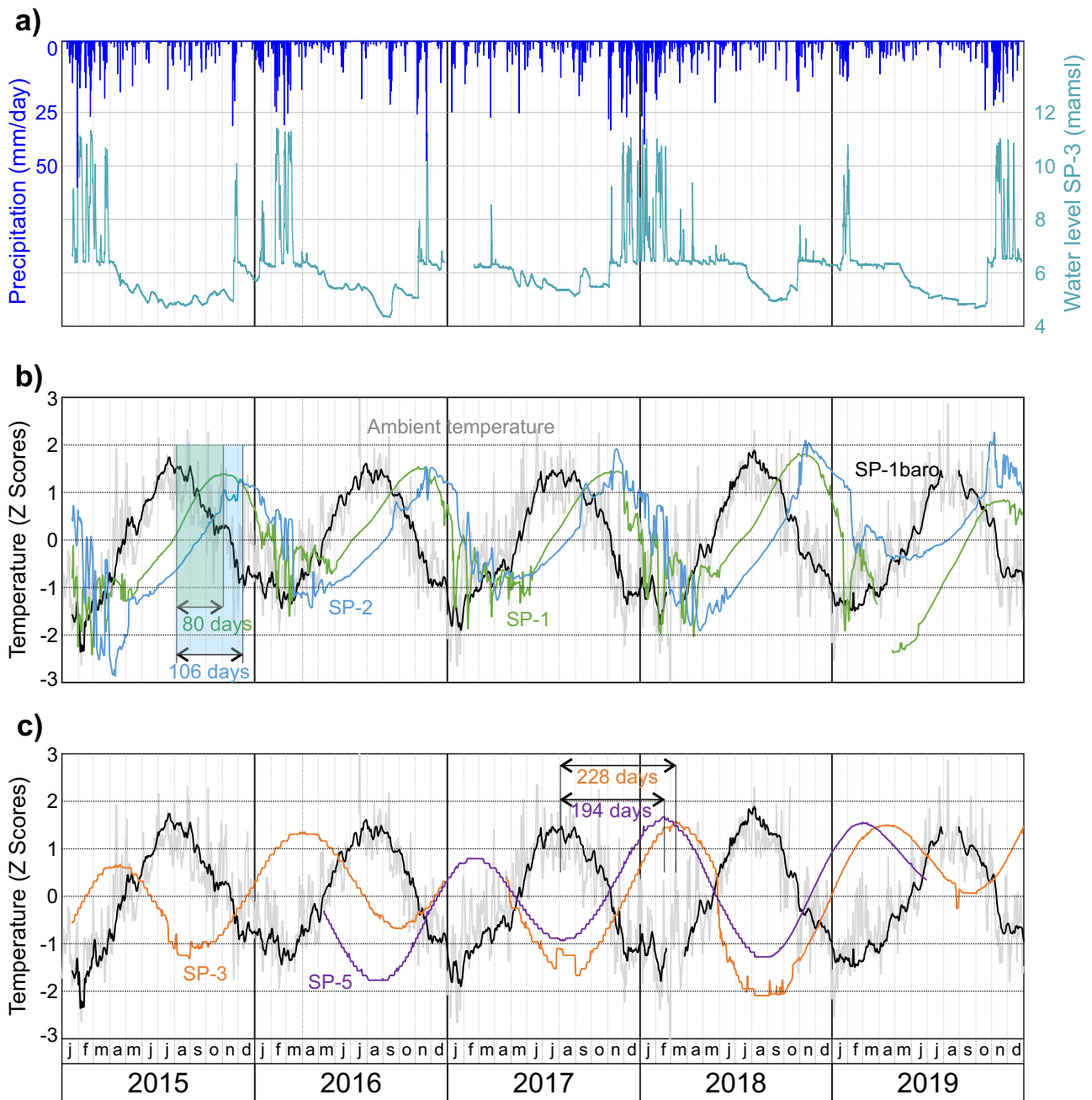
Fig. 7 Hydrometeorological records and temperature evolution inside de rock massif trough piezometers groundwater monitoring: **a** precipitation at Punta Galea meteorological station and groundwater level at piezometer SP-3; **b** comparison between ambient and air temperature recorded at the barometric device placed 20 cm depth in SP-1 and temperatures registered in the piezometers SP-1 and SP-2; **c** comparison with temperatures registered in the piezometers SP-3 and SP-5

of 19.4 m (SP-3) and 21.7 m (SP-5) in the piezometers of the upper terrace of the building exhibit lags of 228 and 194 days (Fig. 7c), respectively, in their temperature signals, which are not significantly affected by rainfall water. In this regard, even though the water level recorded by piezometer SP-3 is clearly influenced by the arrival of rainfall waters (Fig. 7a), the location of the CTD-diver in the practically impervious bottom of the piezometer (Uriarte et al. 2020) minimizes its thermal response. These temperature offsets, evidenced through piezometer water, are much larger than those reported by Mulas et al. (2020) in fissure clayey fillings at depths of up to 1 m and show a complex thermal context in which contraction and dilation processes differentially affect the materials as a function of depth. The final

result in extensometer EXT-1 is a practically inverse evolution with respect to the ambient temperature and to some extent directly proportional to the temperature recorded by piezometer SP-3 (Fig. 6b).

Finally, in Fig. 6c, we show the records from extensometer EXT-2, located in the "Tholos" (Fig. 5), those corresponding to the rod anchored between 8.00 and 8.75 m (long rod) and those corresponding to the rod anchored between 2.5 and 3.25 m (short rod), together with the temperature evolution recorded in the piezometer SP-5. The displacements show a markedly cyclical behavior, with a peak-to-peak amplitude of 0.578 mm for the long rod and of

0.380 mm for the short one. The largest elongation is once again recorded during the winter months, with a moderate offset with respect to the signal from extensometer EXT-1, and of the temperature signal recorded by the piezometer SP-5. In any case, an upward trend in the long-term displacement signal of this extensometer can be seen.

Lomb-Scargle spectral analysis results

Once the displacement records were obtained, discriminating reversible temperature effects from irreversible
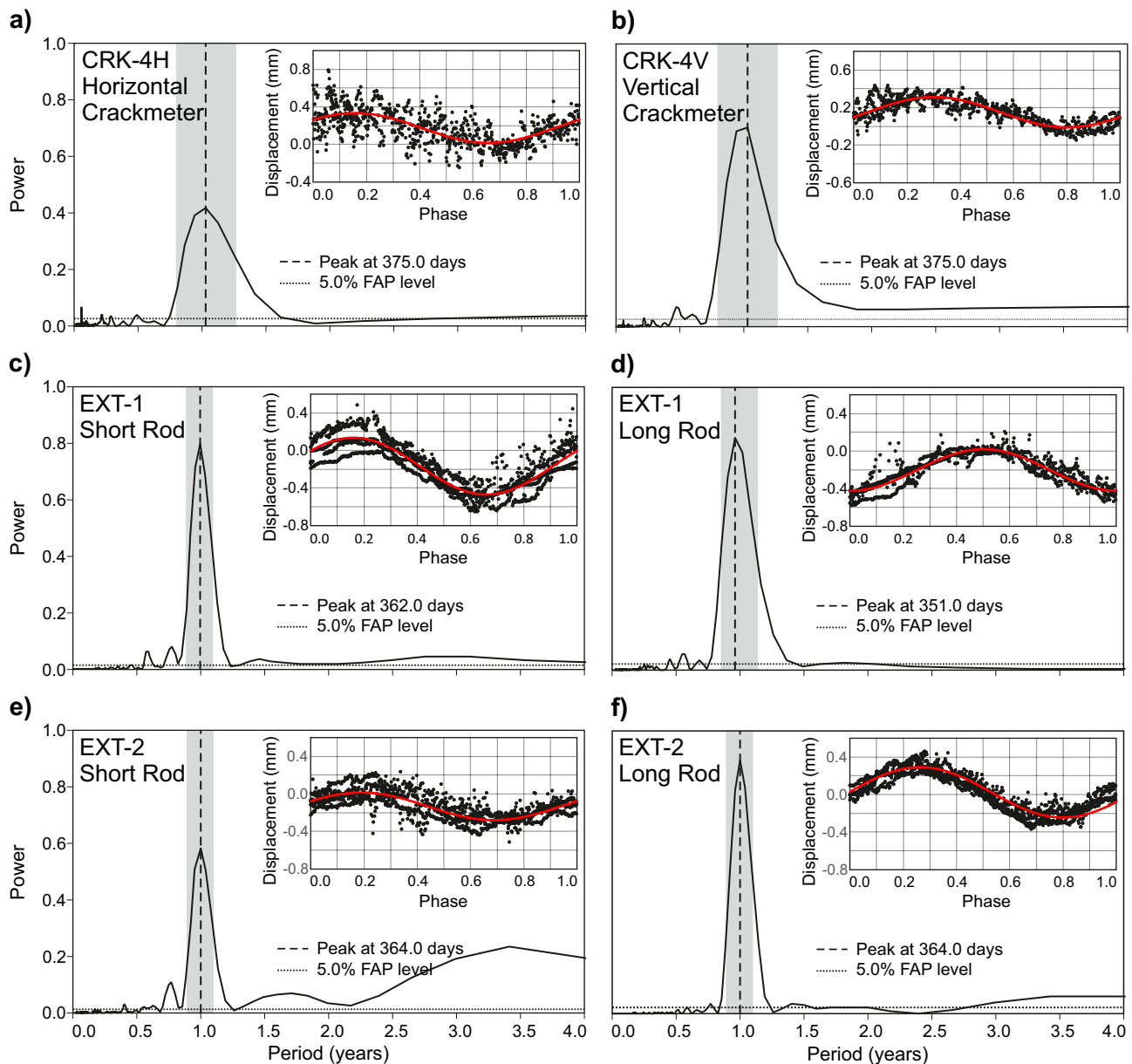
Fig. 8 Periodograms and phase curves for the data series obtained: **a** and **b** horizontal and vertical crackmeters; **c** and **d** extensometer EXT-1 short and long rods; **e** and **f** extensometer EXT-2 short and long rods

damaging effects is required (Bottelin et al. 2013; Weber et al. 2017; Mulas et al. 2020). Since our instruments are exposed to the elements, rainfall and winds produce gaps in the registry of the instrumental records (Fig. 6). To account for this, we introduce the use of the Lomb-Scargle spectral analysis method to analyze the spectral content of the signals, as this technique is particularly well-suited for the analysis of unevenly sampled time series.

Given the difference in the recording rate of the instruments, we used daily averages in all the analyses. First, before calculating the power spectrum of each signal, we did a least-squares linear fit to the raw data. After signal detrending and demeaning, the spectral power analysis allowed us to recognize the most representative periods in the data series. The spectral analysis results along with the phase curves of all the signals are shown in Fig. 8. In Table 1, we show the values of both the linear fits used to detrend the raw data as well as the parameters of the sinusoidal fits derived from the spectral analysis.

As can be seen from Fig. 8, all of the periodograms show a clear peak around 365 days, with spectral peaks between 0.4 and 0.8. These peaks are particularly well defined for the two EXT-1 rods and for the long rod of EXT-2. For the crackmeter signals, the peaks are broader due in part to the lowest number of cycles available in the registry as shown in Fig. 6. In addition to this, for the crackmeter CRK-4H and the short rod of extensometer EXT-2, the main peak height is lower due to the large dispersion of the data, as can be seen in the corresponding phase curves. However, for all cases, the annual periodicity derived from the main peak is highly significant. In this sense, the precision with which a peak's period (or frequency) can be identified is directly related to the width of the peak and often the half-width at half-maximum is used (Vanderplas 2018). The peak width would be the inverse of the observational baseline, which is somewhat different for all our signals. The precision of the periods in our periodograms is marked by the shaded vertical region in Fig. 8. The figure also shows the line corresponding to the 5% false alarm probability (FAP) level

calculated using the Baluev (2008) method. This is the typical approach to quantify the significance of a peak in a periodogram, as it represents the probability that a series with no signal would lead to a peak of similar magnitude. It gives an estimate of the level that corresponds to a 5% false alarm probability for the largest peak, assuming a null hypothesis of non-varying data with Gaussian noise.

In addition to the clear annual period, there are other peaks that are less significant. At periods shorter than the main annual period, these peaks are a combination of harmonics of the annual signal as well as high-frequency noise. Some other peaks, like the one found around 3 and a half years present in the EXT-2 spectra, are too broad to be significant, despite being above the FAP level, and are associated with periodicities in the signal residuals. Finally, other imprecise peaks, like the one between 1.5 and 2 years in the same EXT-2 spectra, would be caused by aliases of the main seasonal signal with periodicities introduced by gaps in the data series.

The values of the main periods ($P_{LS} = 1/f$) derived from this method for the main peaks range from 364 to 375 days (Table 1). The values of the amplitude (A_f) range from lows of about 0.16 mm in the crackmeter CR-4 to highs of about 0.305 mm in the extensometer EXT-1 long rod. The peak-to-peak amplitude values ($A_{p-p} = 2A_f$) are slightly lower to the ones previously derived directly from the experimental data ($A_{p-p \, \exp}$).

From this information, we plotted two new sets of figures: Fig. 9, which shows the evolution of the signals before and after removing the linear trend, together with the sinusoidal fits; and Fig. 10, which shows the permanent displacements not explained by the seasonal variation, after removing the sinusoidal trend. With this detrended series, further least-squares linear fits were made, whose slopes, as expected, were very close to those obtained from the raw data (Table 1). These complementary figures facilitate the interpretation of the information contained in the records, highlighting the non-reversible component of the signals that informs about the active instability process.

Table 1 Parameters of fits to the displacement signals. $P_{LS}(\frac{1}{f})$ is the period determined through power spectrum analysis; A_0 and A_f are the mean value and amplitude of the signals derived from sinusoidal fits to Eq. (1) above; A_{p-p} is the peak-to-peak amplitude, obtained as $2A_f$, and $A_{p-p\exp}$ are the values obtained directly from the raw data. The first column (Lin slope) shows the slope of the linear fit to the raw data, while the last column (Lin slope detr) shows the slope after detrending the sinusoidal fit

| Signal	Lin slope (mm/year)	P_{LS} (days)	A_0 (mm)	A_f (mm)	A_{p-p} (mm)	$A_{p-p\exp}$ (mm)	Lin slope detr (mm/year)
CRK-4H	0.05	375	0.174	0.158	0.316	0.566	0.07
CRK-4 V	−0.13	375	0.151	0.161	0.322	0.403	−0.09
EXT-1 short	−0.03	362	−0.167	0.305	0.610	0.723	−0.01
EXT-1 long	−0.03	351	−0.200	0.223	0.446	0.533	−0.02
EXT-2 short	0.11	364	−0.133	0.148	0.296	0.380	0.11
EXT-2 long	0.10	364	0.022	0.269	0.538	0.578	0.12
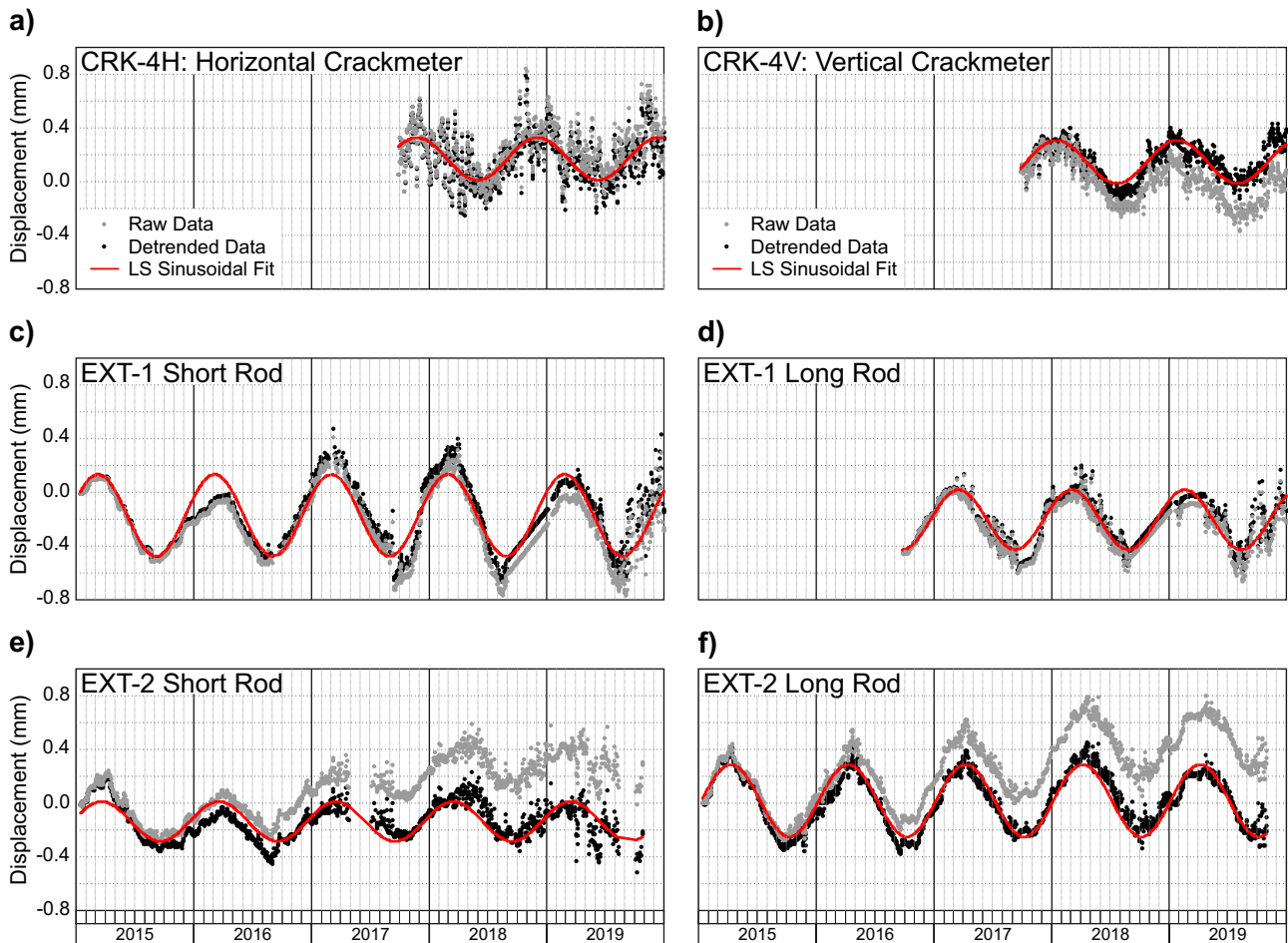
Fig. 9 Raw data (in gray) and detrended data (in black) for the different signals: **a** and **b** horizontal and vertical crackmeters; **c** and **d** extensometer EXT-1 short and long rods; **e** and **f** extensometer EXT-2 short and long rods. The red line shows the sinusoidal fit to the detrended data with the period found through the spectral analysis

Extent of instabilities

Thus, Fig. 9a and b and more clearly Fig. 10a and b show a slow irreversible trend in the evolution of the façade's main crack monitored in the sector where the Southwest Gallery widens (Fig. 5c). It displays a slight opening of the horizontal crackmeter (0.07 mm/year) and a closing tendency from the vertical one (−0.09 mm/year). Two main things to highlight from these figures are as follows: first, the very low magnitude of the irreversible plastic deformation with respect to the peak-to-peak amplitude of the seasonal displacements, which are slightly over 0.3 mm (Table 1); second, the lack of specific seasonal moments of acceleration in the detrended signals, which show a linear tendency (Fig. 9a, b). Regarding the stability of this sector of the building, the observed trends imply a very slowly sinking and moving outward motion of the outermost element of the southwest façade. This motion is consistent with the slight expansion (0.12 mm/year) recorded by the long

rod of extensometer EXT-3, which is located as shown in Fig. 3; it should be noted, at this point, that its short rod was only functioning during the first year of monitoring (14/06/2016–19/09/2017). Contextualizing all this information into the observations of this sector, the origin of the instability would be in the intermediate pillars that were built directly on the original cliff (Fig. 2f) and more precisely in the intermediate pillar that is located underneath the stairs that give access to the upper terrace (Fig. 5). The greater load of this pillar breaks the superficial stratum locally and produces a slight descending displacement towards the exterior of the building. This motion is jointly transmitted by the concrete structure producing the traction crack in the staircase of the upper terrace (Fig. 5b) and the detachment of the upper part of the facade with respect to the base of the building, which is directly grounded on the underlying terrain. Even though the irreversible component of the displacement is small, it does imply an active plastic deformation, which calls for the need to reinforce the supports of the
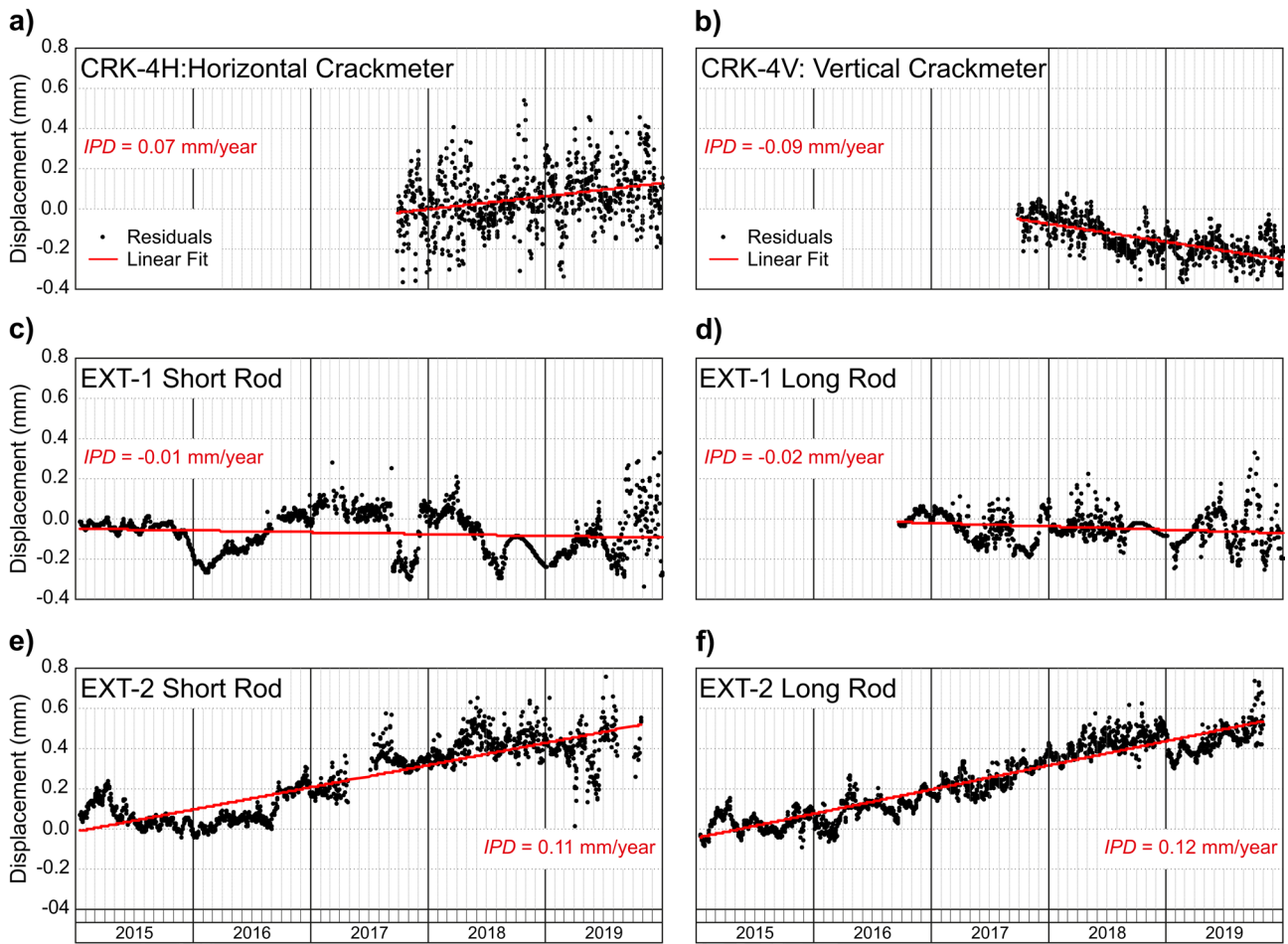
Fig. 10 Residuals after detrending the sinusoidal fit: **a** and **b** horizontal and vertical crackmeters; **c** and **d** extensometer EXT-1 short and long rods; **e** and **f** extensometer EXT-2 short and long rods. The red line shows the linear fit corresponding to the non-reversible plastic displacement

intermediate pillars. In any case, the rocky massif as a whole is stable, not developing pressure on the structure.

Referring to the data from extensometer EXT-1, it shows a similar tendency for the short and long rods, with a clearly marked seasonal component (Fig. 9c, d). The displacements after removing the cyclic component (Fig. 10c, d) show that there is almost no irreversible plastic deformation since the slopes are barely −0.01 mm/year for the short rod and −0.02 mm/year for the long rod. This behavior, indicative of a stable environment in the Northwest Gallery, is consistent with the rest of the observations in this part of the building, including those from the inclinometer INC-1, which does not show any movement. Regarding the crack found in the top slab, it was determined that this was caused by the careless demolition carried out by a backhoe at the upper entrance to the gallery. Thus, the rocky massif as a whole provides a stable support for the building in this sector.

Finally, the data from extensometer EXT-2 show that the short and long rods follow a similar evolution (Fig. 9e, f).

The irreversible plastic displacements, after sinusoidal fit detrending, evidence in this case a clear elongation tendency (Fig. 10e, f) with small but continuous displacement values of 0.11 mm/year for the short rod and 0.12 mm/year for the long rod. Again, it is worth noting the limited amplitude of these movements, compared to the peak-to-peak amplitudes of the seasonal displacements that go from 0.3 mm to slightly over 0.5 mm (Table 1); in addition, after the sinusoidal fit detrending, the signal shows a linear upward trend, without accelerations associated with specific seasonal periods (Fig. 10e, f). The fact that practically all the displacement can be explained by the motion registered in the short rod, which is anchored at a depth between 2.5 and 3.25 m, would indicate that the movement occurs in the outermost environment of the cliff-building complex. Putting into context all the information derived from the observations in this sector, the origin of the instability would be in the different foundation of the "Tholos," whose innermost part is placed directly over the rocky massif, while its outermost part is placed over a cavity and supported only by the perimeter

wall of the façade. With this layout (Fig. 11), the load of the outermost columns of this pavilion causes the subsidence and local cracking of the façade wall and the inner concrete slab. The slight downward movement towards the outside recorded by the extensometer is consistent with apertures of the order of 0.12 mm/year recorded in the cracks of this sector. Also, in this case, even though the irreversible component of the displacement was found to be very small, its dynamics prompts to take action aimed at reinforcing the support of the outermost columns of the pavilion. As in the previous sectors, the rock massif is stable and is not in itself the cause of the existing damage.

Discussion

Monitoring issues

The identification, damage assessment, and evaluation of the exposure of cultural heritage sites to geo-hazards, in order to establish appropriate corrective and conservation measures, are currently a great challenge. To address this challenge, different monitoring techniques including satellite and aerial imagery, satellite and ground-based radar interferometry, laser scanning, total station, and geotechnical networks have proven to be useful to analyze more and more precisely displacements at different scales, ranging from medium-large site scale to local-scale displacements and structural deformations (e.g., Greif et al. 2006; Roje-Bonacci et al. 2014; Margottini et al. 2015; Janeras et al. 2015; Themistocleous et al. 2018; Dal Cin and Russo 2019).
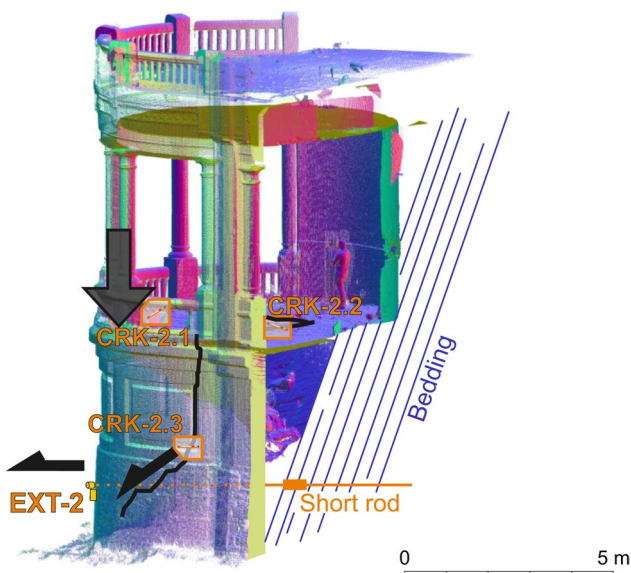
Fig. 11 Movements explanatory diagram at the "Tholos" (explanation in the text)

In the case of extremely slow movements (Greif et al. 2006), geotechnic networks placed on site allow for continuous monitoring with high precision. In this regard, image-based methods can attain sub millimeter precisions, with an accuracy of 0.5–0.7 mm for GB-InSar (Ferrigno et al. 2017), while the extensometers and crackmeters used in this work have an accuracy of ± 0.01 mm (extensometer EXT-1 and EXT-2) to ± 0.05 mm (crackmeters CRK-1 to CRK-4) and ± 0.1 mm (extensometer EXT-3). The main limitation of these devices is their limited spatial reach (Zhu et al. 2017; Themistocleous et al. 2018), while their main advantage is that they allow for the continuous direct record of displacement in short- and long-term scales.

Our records show an evident relationship with temperature. In the case of the most superficial devices, crackmeters, the records display reversible opening-closing seasonal movements characteristic of the materials thermal response to ambient temperature variations (Mentes 2012; Colombero et al. 2018). The extensometers, which measure displacements relative to internal points in the rock massif, show a more complex behavior, with the highest elongations occurring cyclically during the coldest months. This evolution would be related to the offset of the temperature signal in the interior of the rock massif (Bottelin et al. 2013; Mulas et al. 2020). In our work, this thermal signal offset has been recognized by the water temperature records of the hydrogeological monitoring piezometers. At this point, a more detailed analysis of these seasonal evolutions would require a specific monitoring system, e.g., by including temperature sensors at different depths in the extensometric boreholes. In any case, these elastic movements are reversible and would not involve destabilization processes by themselves (Greif et al. 2006; Weber et al. 2017; Mulas et al. 2020).

Lomb-Scargle analysis and damage assessment

The removal of these seasonal reversible evolutions is the starting point to characterize often less marked trends of irreversible nature that condition the stability of the cultural heritage site in the medium-long term. For this purpose, we introduce the use of the Lomb-Scargle analysis to identify seasonal trends in geotechnical data series. This analysis, like the one proposed by Mulas et al. (2020), avoids the bias that the consideration of temperature series (Weber et al. 2017) could introduce in the results, and as Vanderplas (2018) points out, it is the optimal statistic for fitting a sinusoidal model to data. Furthermore, an additional advantage of this methodology is that it allows working with unevenly spaced time series, which is a notable advantage given the considerable exposure to the elements of the measurement equipment that in many cases leads to discontinuous series. In our case, all the periodograms obtained from daily data series showed a clearly marked annual cyclical component,

with the remaining cyclical components not being statistically significant.

Detrending of the signal with the sinusoidal fit derived from the Lomb-Scargle spectral analysis allows to ultimately display the magnitude and temporal evolution of the irreversible damage. In our work, long-term monitoring of movements in the Punta Begoña Galleries shows a clearly differentiated behavior: the Northwest Gallery is stable, while the Southwest Gallery shows evidence of slow continuous displacements in the two monitored sectors, with velocities up to 0.12 mm/year. The small magnitude of these movements, when compared to the seasonal component between 0.3 and 0.5 mm, highlights the need of a continuous monitoring system composed of accurate geotechnical devices. These movements are not related to instability processes of the massif, which appears stable, but to local support problems of the building structure. In addition, the records do not show movement accelerations associated with specific weather events, displaying the residuals a linear tendency.

Overall, the Lomb-Scargle analysis proved to be a particularly well-suited tool for the analysis of long-term geotechnical records at cultural heritage sites. Its applicability, to analyze and characterize movements in environments where accelerations associated with specific seasonal events (such as snowmelt, freeze–thaw cycles or intense rainfall periods, e.g., D'Amato et al. (2016); Frayssines and Hantz (2006); Sandersen et al. (1997)) give rise to steps in the signal of residuals, remains to be investigated.

Conclusions

The monitoring of long-term structural movements in the most compromised sectors of the Punta Begoña Galleries and the processing of the data series through Lomb-Scargle spectral analysis have allowed us to recognize the nature of damage and its temporal evolution in this building sited on a coastal cliff.

The main advantage of the Lomb-Scargle spectral analysis is that it allows work with unevenly spaced data series to facilitate the identification of periodic components in the signals. From this, it is possible to recognize the role of seasonal patterns in the measurements and to understand the long-term evolution of the series, differentiating reversible elastic movements from irreversible plastic ones.

In our case, it has been possible to distinguish the stable behavior of the Northwest Gallery of the building, contrary to the active dynamics of two sectors of the Southwest Gallery. The limited magnitude of the identified irreversible movements (with a maximum of 0.12 mm/year) underscores the need for long-term monitoring for an adequate contextualization of the information. This information is particularly necessary for the recovery of heritage buildings and natural environments that require interventions that respect their values, avoiding irrecoverable losses (Heinemann 2008; Kyriazi 2019; ICOMOS 2014).

Declarations

Conflict of interest The authors declare no competing interests.

References

Baluev RV (2008) Assessing the statistical significance of periodogram peaks. Mon Not Royal Astron Soc 385:1279–1285. https://doi.org/10.1111/j.1365-2966.2008.12689.x

Bottelin P, Lévy C, Baillet L, Jongmans D, Guéguen P (2013) Modal and thermal analysis of Les Arches unstable rock column (Vercors massif, French Alps). Geophys J Int 194:849–858. https://doi.org/10.1093/gji/ggt046

Casula G, Fais S, Ligas P (2009) An experimental application of a 3-D terrestrial laser scanner and acoustic techniques in assessing the quality of the stones used in monumental structures. Int J Microstruct Mater Prop 4:45–56. https://doi.org/10.1504/IJMMP.2009.028432

Cempel C (2003) Multidimensional condition monitoring of mechanical systems in operation. Mech Syst Signal Proc 17:1291–1303. https://doi.org/10.1006/mssp.2002.1573

Chang PC, Flatau A, Liu SC (2003) Health monitoring of civil infrastructure. Struct Health Monit 2:257–267. https://doi.org/10.1177/1475921703036169

Colombero C, Comina C, Vinciguerra S, Benson PM (2018) Microseismicity of an unstable rock mass: from field monitoring to laboratory testing. J Geophys Res: Solid Earth 123:1673–1693. https://doi.org/10.1002/2017JB014612

Colomina I, Molina P (2014) Unmanned aerial systems for photogrammetry and remote sensing: a review. ISPRS J Photogramm Remote Sens 92:79–97. https://doi.org/10.1016/j.isprsjprs.2014.02.013

Custance-Baker A, Macdonald S (2014) Conserving concrete heritage, Experts meeting. Meet Rep. The Getty Conservation Institute, Los Angeles

Dal Cin A, Russo S (2019) Evaluation of static and dynamic long-term structural monitoring for monumental masonry structure. J Civ Struct Health Monit 9:169–182. https://doi.org/10.1007/s13349-019-00324-z

Damas Mollá L, Uriarte JA, Aranburu A, Bodego A, Balciscueta U, García Garmilla F, Morales T (2018) Systematic alteration survey and stone provenance for restoring heritage buildings: Punta Begoña Galleries (Basque-Country, Spain). Eng Geol 247:12–26. https://doi.org/10.1016/j.enggeo.2018.10.009

Damas Mollá L, Sagarna Aranburu M, Uriarte JA, Aranburu A, Zabaleta A, García-García F, Antigüedad I, Morales T (2020) Understanding the pioneering techniques in reinforced concrete: the case of Punta Begoña Galleries, Getxo, Spain. Build Res Inf 48:785–801. https://doi.org/10.1080/09613218.2019.1702498

D'Amato J, Hantz D, Guerin A, Jaboyedoff M, Baillet L, Mariscal A (2016) Nat Hazards Earth Syst Sci 16:719–735. https://doi.org/10.5194/nhess-16-719-2016

De Stefano A, Matta E, Clemente P (2016) Structural health monitoring of historical heritage in Italy: some relevant experiences. J Civ Struct Health Monit 6:83–106. https://doi.org/10.1007/s13349-016-0154-y

Díaz Morlán P (1999) Horacio Echevarrieta, 1870–1963: el capitalista republicano. LID Editorial Empresarial, Madrid

Díaz Morlán P (2011) Horacio Echevarrieta, empresario republicano (Bilbainos Recuperados). Muelle de Uribitarte Editores, Bilbao

Ding X, Ren D, Montgomery B, Swindells C (2000) Automatic monitoring of slope deformations using geotechnical instruments. J Surv Eng 126:2. https://doi.org/10.1061/(ASCE)0733-9453(2000)126:2(57)

Dong Z, Liang F, Yang B, Xu Y, Zang Y, Li J, Wang Y, Dai W, Fan H, Hyyppä J, Stilla U (2020) Registration of large-scale terrestrial laser scanner point clouds: a review and benchmark. ISPRS J Photogramm Remote Sens 163:327–342. https://doi.org/10.1016/j.isprsjprs.2020.03.013

Ferrigno F, Gigli G, Fanti R, Intrieri E, Casagli N (2017) GB-InSAR monitoring and observational method for landslide emergency management: the Montaguto earthflow (AV, Italy). Nat Hazards Earth Syst Sci 17:845–860. https://doi.org/10.5194/nhess-17-845-2017

Frayssines M, Hantz D (2006) Failure mechanisms and triggering factors in calcareous cliffs of the Subalpine Ranges (French Alps). Eng Geol 86:256–270. https://doi.org/10.1016/j.enggeo.2006.05.009

Greif V, Sassa K, Fukuoka H (2006) Failure mechanism in an extremely slow rock slide at Bitchu-Matsuyama castle site (Japan). Landslides 3:22–38. https://doi.org/10.1007/s10346-005-0013-0

Guo Q, Wang X, Zhang H, Li Z, Yang S (2009) Damage and conservation of the high cliff on the Northern area of Dunhuang Mogao Grottoes, China. Landslides 6:89–100. https://doi.org/10.1007/s10346-009-0152-9

Heinemann HA (2008) Why historic concrete buildings need holistic surveys. In: Walraven J, Stoelhorst D (eds) Tailor made concrete structures. Taylor & Francis Group, London, pp 103–108

Heinemann HA (2013) Historic concrete: from concrete repair to concrete conservation. Dissertation, University of Dortmund. https://doi.org/10.4233/uuid:987fafd0-cd76-4230-be0e-be8843cae08e

Hocke K, Kämpfer N (2009) Gap filling and noise reduction of unevenly sampled data by means of the Lomb-Scargle periodogram. Atmos Chem Phys 9:4197–4206. https://doi.org/10.5194/acp-9-4197-2009

ICOMOS (International Council on Monuments and Sites) (2003) Principles for the analysis, conservation and structural restoration of architectural heritage. ICOMOS 14th General Assembly, Victoria Falls

ICOMOS (International Council on Monuments and Sites) (2010) Illustrated glossary on stone deterioration patterns. ICOMOS International Scientific Committee for Stone, Paris

ICOMOS (International Council on Monuments and sites) (2014) Approaches for the conservation of twentieth century architectural heritage. ICOMOS International Scientific Committee on 20th Century Heritage, Madrid

Janeras M, Jara JA, López F, Marturià J, Royán MJ, Vilaplana JM, Aguasca A, Fàbregas X, Cabranes F, Gili JA (2015) Using several monitoring techniques to measure the rock mass deformation in the Montserrat Massif. International Symposium on Geohazards and Geomechanics. IOP Conf Ser: Earth Environ Sci 26:012030. https://doi.org/10.1088/1755-1315/26/1/012030

Janeras M, Jara JA, Royán MJ, Vilaplana JM, Aguasca A, Fàbregas X, Gili JA, Buxó P (2017) Multi-technique approach to rockfall monitoring in the Montserrat massif (Catalonia, NE Spain). Eng Geol 219:4–20. https://doi.org/10.1016/j.enggeo.2016.12.010

Kyriazi E (2019) Façadism, building renovation and the boundaries of the authenticity. Aesthet Investig 2:184–195. https://doi.org/10.5281/zenodo.4073206

Laborde Marqueze A (2013) COREMANS project: "Criteria for working in stone materials". Ministerio de Educación, Cultura y Deporte, Madrid

Lomb NR (1976) Least-squares frequency analysis of unequally spaced data. Astrophys Space Sci 39:447–462. https://doi.org/10.1007/BF00648343

Margottini C, Antidze N, Coromins J, Crosta GB, Frattini P, Gigli G, Giordan D, Iwasaky I, Lollino G, Manconi A, Marinos P, Scavia C, Sonnessa A, Spizzichino D, Vacheishvili N (2015) Landslide hazard, monitoring and conservation strategy for the safeguard of Vardzia Byzantine monastery complex, Georgia. Landslides 12:193–204. https://doi.org/10.1007/s10346-014-0548-z

McKinney W (2010) Data structures for statistical computing in Python. Proc 9th Python Sci Conf. SciPy, Austin, pp 56–61

Mentes G (2012) A new borehole wire extensometer with high accuracy and stability for observation of local geodynamic processes. Rev Sci Instrum 83:015109. https://doi.org/10.1063/1.3676652

Montuori A, Luzi G, Stramondo S, Casula G, Bignami C, Bonali E, Bianchi MG, Crosetto M (2014) Combined use of ground-based systems for Cultural Heritage conservation monitoring. Proc Geosci Remote Sens Symp (IGARSS). IEEE International, Québec, pp 4086–4089. https://doi.org/10.1109/IGARSS.2014.6947384

Morales T, Uribe-Etxebarria G, Uriarte JA, Fernández de Valderrama I (2004) Geomechanical characterisation of rock masses in Alpine regions: the Basque Arc (Basque-Cantabrian basin, Northern Spain). Eng Geol 71:343–362. https://doi.org/10.1016/S0013-7952(03)00160-1

Mulas M, Marnas M, Ciccarese G, Corsini A (2020) Sinusoidal wave fit indexing of irreversible displacements for crackmeters monitoring of rockfall areas: test at Pietra di Bismantova (Northern Apennines, Italy). Landslides 17:231–240. https://doi.org/10.1007/s10346-019-01248-x

Pardo-Igúzquiza E, Rodríguez-Tovar FJ (2011) Implemented Lomb-Scargle periodogram: a valuable tool for improving cyclostratigraphic research on unevenly sampled deep sea stratigraphic sequences. Geo-Mar Lett 31:537–545. https://doi.org/10.1007/s00367-011-0247-x

Pardo-Igúzquiza E, Rodríguez-Tovar FJ (2012) Spectral and cross-spectral analysis of uneven time series with the smoothed Lomb-Scargle periodogram and Monte Carlo evaluation of statistical significance. Comput Geosci 49:207–216. https://doi.org/10.1016/j.cageo.2012.06.018

Park J, Lindberg C, Vernon FL (1987) Multitaper spectral analysis of high-frequency seismograms. J Geophys Res Atmos 921:12675–12684. https://doi.org/10.1029/JB092iB12p12675

Pestiaux P, Berger A (1984) An optimal approach to the spectral characteristics of deep-sea climatic records. In: Berger A, Imbrie J, Hays J, Kukla G, Saltzman B (eds) Milankovitch and climate. D. Reidel Publ. Co., Dordrecht, pp 417–445

Press WH, Rybicki GB (1989) Fast algorithm for spectral analysis of unevenly sampled data. Astrophys J 338:277–280. https://doi.org/10.1086/167197

Reback J, the *pandas* development team (2020, March 18) pandas-dev/pandas: Pandas 1.0.3. Zenodo. https://doi.org/10.5281/zenodo.3715232

Roje-Bonacci T, Miščević P, Salvezani D (2014) Non-destructive monitoring methods as indicators of damage cause on Cathedral of St. Lawrence in Trogir. Croatia J Cult Herit 15:424–431. https://doi.org/10.1016/j.culher.2013.07.008

Rosell J, Cárcamo J (1994) La Fábrica CERES de Bilbao. Los orígenes del hormigón armado y su introducción en Bizkaia. Colegio Oficial de Aparejadores y Arquitectos Técnicos de Bizkaia, Bilbao.

Sandersen F, Bakkehøi S, Hestnes E, Lied K (1997) The influence of meteorological factors on the initiation of debris flows, rockfalls, rockslides and rockmass stability. In: Senneset K (ed) Landslides vol 3: Proc 7th Int Symp Landslides, 3rd edn. AA Balkema, Trondheim, pp 97–114

Scargle JD (1982) Studies in astronomical time series analysis. II. Statistical aspects of spectral analysis of unevenly spaced data. Astrophys J 263:835–853. https://doi.org/10.1086/160554

Schulz M, Stattegger K (1997) Spectrum: spectral analysis of unevenly spaced paleoclimatic time series. Comput Geosci 23:929–945. https://doi.org/10.1016/S0098-3004(97)00087-3

Tang P, Chen F, Zhu X, Zhou W (2016) Monitoring cultural heritage sites with advanced multi-temporal InSAR technique: the case study of the Summer Palace. Remote Sens 8:432. https://doi.org/10.3390/rs8050432

Themistocleous K, Danezis C, Frattini P, Crosta G, Valagussa A (2018) Best practices for monitoring, mitigation and preservation of cultural heritage sites affected by geo-hazards: the results of the PROTHEGO project. Sixth International Conference on Remote Sensing and Geoinformation of the Environment. https://doi.org/10.1117/12.2503915

Themistocleous K, Danezis C (2019) Monitoring Cultural Heritage Sites affected by geo-hazards using in situ and SAR data: the Choirokoitia case study. In: Hadjimitsis DG, Themistocleous K, Cuca B, Agapiou A, Lysandrou V, Lasaponara R, Masini N, Schereier G (eds) Remote sensing for archaeology and cultural landscapes. Springer, Cham, pp 285–308. https://doi.org/10.1007/978-3-030-10979-0_16

Uriarte JA, Damas Mollá L, Sagarna M, García F, Antigüedad I, Morales T (2020) Characterization of complex groundwater flows in the environment of singular buildings by combining hydrogeological and non-destructive geophysical (ground-penetrating radar) techniques: Punta Begoña Galleries (Getxo, Spain). Hydrol Process 34:1004–1015. https://doi.org/10.1002/hyp.13635

VanderPlas JT, Ivezić Z (2015) Periodograms for multiband astronomical time series. Astrophys J 812:18. https://doi.org/10.1088/0004-637X/812/1/18

VanderPlas JT (2018) Understanding the Lomb-Scargle Periodogram. Astrophys J Suppl Ser 236:16. https://doi.org/10.3847/1538-4365/aab766

Vaughan S, Bailey RJ, Smith DG (2015) Cyclostratigraphy: data filtering as a source of spurious spectral peaks. Geol Soc London Spec Publ 404:151–156. https://doi.org/10.1144/SP404.11

Weber S, Beutel J, Faillettaz J, Hasler A, Krautblatter m, Vieli A, (2017) Quantifying irreversible movements in steep, fractured bedrock permafrost on Matterhorn (CH). Cryosph 11:567–583. https://doi.org/10.5194/tc-11-567-2017

Weedon G (2003) Time-series analysis and cyclostratigraphy: examining stratigraphic records of environmental cycles. Cambridge University Press, Cambridge. https://doi.org/10.1017/CBO9780511535482

Zhu H-H, Shi B, Zhang C-C (2017) FBG-based monitoring of Geohazards: current status and trends. Sensors 17:452. https://doi.org/10.3390/s17030452